ELSEVIER

Polymer 42 (2001) 281–287

polymer

www.elsevier.nl/locate/polymer

On the structure of the phase A of comb-like poly(α-alkyl-β,L-aspartate)s: a molecular modelling study

D. Zanuy, A.M. Namba[1], S. León, C. Alemán*, S. Muñoz-Guerra

Departament d'Enginyeria Química, E.T.S. d'Enginyers Industrials de Barcelona, Universitat Politècnica de Catalunya, Diagonal 647, Barcelona E-08028, Spain

Received 14 January 2000; received in revised form 29 February 2000; accepted 12 April 2000

Abstract

The phase A of the comb-like poly(α-*n*-octadecyl-β,L-aspartate) has been investigated using atomistically detailed computer simulations. Four independent polymer chains of 13 residues were constructed and packed in an orthogonal simulation box with periodic continuation conditions. A set of microstructures was obtained by Configurational Bias Monte Carlo generation. Some torsional angles of the alkyl side chains were constrained in order to facilitate the crystallization of paraffinic chains. The resulting microstructures have provided a detailed description of the structural behaviour of this phase allowing to characterize some related properties. The most relevant results have been compared with those recently obtained for the phase B and with the available experimental data.

Keywords: Poly(α-alkyl-β,L-aspartate); Molecular modelling; Comb-like polymers

1. Introduction

Some years ago a great effort was devoted to study comb-like poly(γ-alkyl-α,L-glutamate)s, [1–5] i.e. poly(α,L-glutamate)s bearing long alkyl side chains, abbreviated PALG-*n*, *n* being the number of carbon atoms contained in the alkyl group. These polypeptides form biphasic structures when the alkyl side chain is long enough, [2] i.e. $n > 10$. In these structures, the polypeptide α-helix main chains are arranged in layers with side chains crystallized in a separated phase, which is located between the layers. They present two transition temperatures T_1 and T_2 ($T_1 < T_2$) which correspond to the melting of the side chains and to the interconversion between two liquid-crystal-like structures, respectively [1,2,5].

More recently, a new family of comb-like polypeptides constituted by β-amino acids has emerged [6–9]. These are the poly(α-alkyl-β,L-aspartate)s, abbreviated PAALA-*n*, which can be considered as stereoregular nylon 3 derivatives bearing an alkoxy-carbonyl group attached to the backbone β-carbon of the repeating unit.

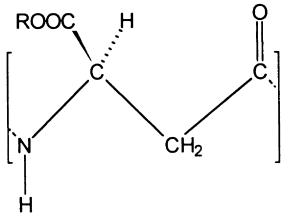

Compounds with $n = 12$, 14, 16, 18 and 22 were synthesized and their structure in the solid state examined by i.r. dichroism, NMR and X-ray diffraction [6,7]. All of them adopt a 13/4 helical conformation stabilized by intramolecular hydrogen bonds, which is the conformation usually observed for the poly(β,L-aspartate)s bearing short alkyl side chains [10,11]. These comb-like PAALA-*n* present biphasic structures similar to those previously described for PALG-*n* with $n > 10$. Thus, three different phases, namely A, B and C (Fig. 1), can be observed for these compounds upon increasing temperature, the 13/4 helical conformation being retained through the whole sequence of transitions.

At temperatures below T_1 a smectic-like phase, denoted phase A, is observed. This is conceived as a structure with the helices aligned in layers separated by the crystallized side-chains [6]. X-ray and electron diffraction, and DSC

* Corresponding author. Tel.: +34-93401-6680/6681; fax: +34-93401-6600/7150.

E-mail address: aleman@eq.upc.es (C. Alemán).

[1] Present Address: Departamento de Química da Faculdade de Filosofia, Ciências e Letras de Ribeirão Preto, Universidade de São Paulo, Avenida Bandeirantes No. 3900, 14049-901, Ribeirão Preto, SP, Brazil.

0032-3861/01/$ - see front matter
PII: S0032-3861(00)00313-X

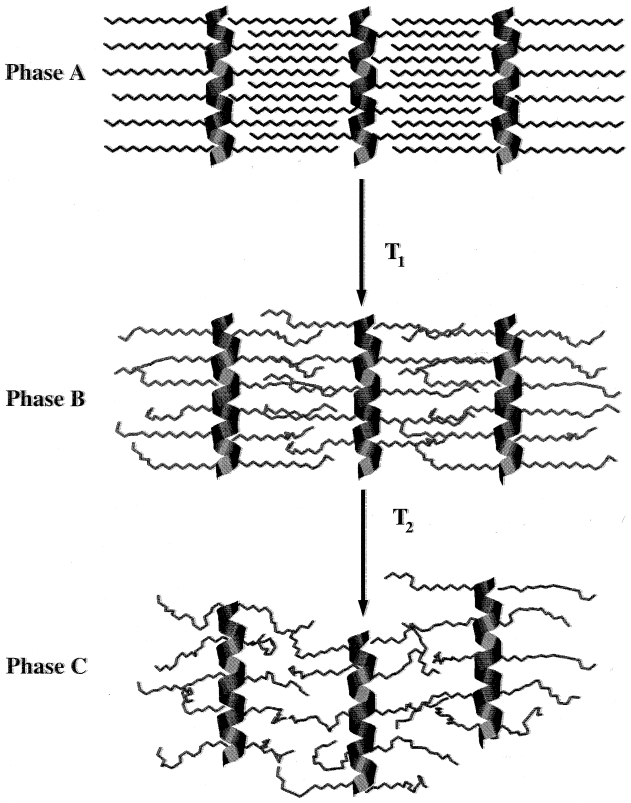

Fig. 1. Schematic model illustrating the structural changes that take place in PAALA-*n* with $n \geq 12$ by the effect of temperature.

measurements indicate a hexagonal arrangement of the side chains similar to the hexagonal crystal phase exhibited by *n*-alkanes at temperatures near their melting points [12]. It should be emphasized that this situation differs from that observed in PALG-*n* with $n > 10$, in which the side chains crystal lattices resemble the triclinic unit cell displayed by low molecular weight *n*-alkanes or polyethylene [2]. The phase B of PAALA-*n* with $n \geq 12$ is obtained upon heating above T_1 and converts into phase C upon heating above T_2. In phase B, the helices retain the layered arrangement but the alkyl side chains are in a disordered state due to the melting of the paraffin crystallites [6,7]. Finally, phase C has been interpreted to consist of an uniaxial arrangement of independent helices embedded in a matrix made up of side chains in a nearly coiled state.

The phase B of PAALA-*n* with *n* ranging from 12 to 18 was recently investigated using Monte Carlo (MC) simulations of an atomistically explicit model [9]. The results provided a detailed description of the structural behaviour of the poly(β-L-aspartate)s in this cholesteric phase. Furthermore, the ability of phase B of PAALA-*n* to mimic barrier synthetic composites and biological structures related with the permeation processes was also investigated by studying both the distribution of the unoccupied space and the solubility of small gaseous penetrants [7]. Whereas the phase B has been characterized in detail, the structure of phase A has not been examined at the atomistic level. This is a serious shortcoming since a detailed understanding of the structure is a crucial point to have a complete view of the transition that takes place when phase A changes to phase B [6].

In this work, we present a molecular modelling study on the phase A of PAALA-*n* with $n \geq 12$ using MC simulations. Thus, the goal of this work is to describe the most important structural properties of the phase A and to compare them with those of the phase B. We have concentrated our efforts on PAALA-18 which is the most representative member of the comb-like PAALA-*n* series and that has been studied in detail by experimental methods.

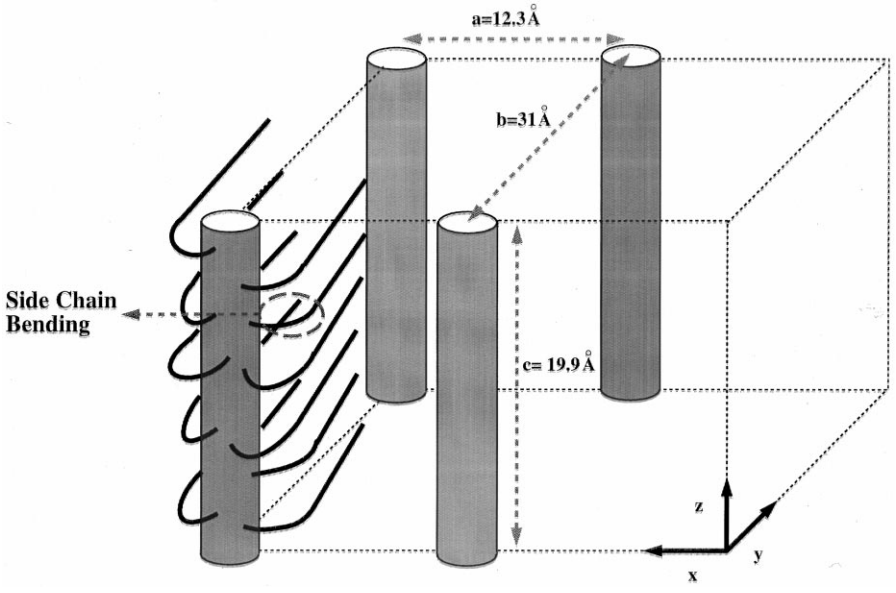

Fig. 2. Schematic representation of the simulated model. The lattice dimensions are indicated and only the four parent helices are represented.

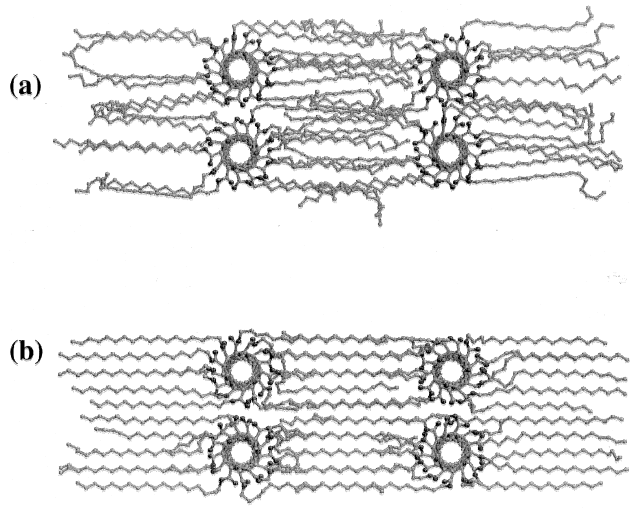

Fig. 3. Representative structure of the PAALA-18 obtained after NVT equilibration considering: (a) all the dihedral angles of the alkyl side chains as degrees of freedom; and (b) three central torsional angles of the alkyl side chains fixed at *trans* conformation and the remainders left free.

2. Methods

2.1. Construction of the simulated model.

The starting geometry for the layered structure of PAALA-18 was built using the available experimental information [6]. The helical conformation used for the polymer under study was generated using the conformational parameters obtained for other poly(α-alkyl-β,L-aspartate)s bearing small alkyl side chains [10,11]. The conformation is a right-handed 13/4 helix with 3.25 residues per turn and an axial repeat length of $c_o = 19.9$ Å. The torsional angles of the helix backbone were kept constant at the values reported in Ref. [10]. Four independent helices were packed in an orthogonal simulation box with the helix axes oriented parallel to the *z*-axis (Fig. 2). Helices were arranged antiparallel with respect to each other as was previously observed for PAALA-*n* with $n \leq 8$ [8,10,11]. The torsional angles associated to the methylene units of the alkyl side chains were initially considered in *trans* conformation with the exception of those located between two helices within a layer, i.e. the torsional angles involved in the side chain bending (Fig. 2), which were taken from our previous simulations for the phase B of PAALA-18 [7,9].

The distance between the helices within a layer, i.e. the box edge *a* along the *x*-axis, was fixed at 12.3 Å, which is the value determined from X-ray diffraction [6], and was kept constant along the simulations. The distance between the layers, i.e. the box edge *b* along the *y*-axis, was initially fixed at 36 Å and was progressively reduced to 31 Å (see below), which is the observed value. Therefore, the degrees of freedom in the simulations were the torsional angles of the alkyl side groups and the setting angle of each chain, i.e. the rotation angle around the *z*-axis.

2.2. Computational procedure

The phase A of PAALA-18 was simulated using an advanced MC sampling technique (Continuum Configurational Bias, CCB-MC) [13,14]. The CCB method consists of the following three steps: (i) a chain is selected at random; (ii) the chain is cut at a random position; (iii) the chain is sequentially regrown. The chain is regrown bond-by-bond by examining a number of possible position, which are chosen randomly. In order to ensure the condition of microscopic reversibility an appropriate transition probability is chosen [13,14]. This method was initially developed to be efficient in the study of dense systems and has been successfully used in the simulations of the crystal structure of PAALA-4 [15] and the phase B of PAALA-n with $n \geq 12$ [7,9]. It should be emphasized that the aim of this work is to obtain an atomistic model for the phase A of PAALA-18. Accordingly, the available experimental information [6] has been used to restrict the simulations to the desired phase, as will be discussed below.

Since the box used in the simulations consists of four independent chains of 13 residues, a typical simulation deals with 1404 atoms. All the simulations were of NVT type ($T = 298$ K) considering both periodic continuation conditions and the minimum-image convention. Initially, the box edge *b* along the *y*-axis was slowly driven from 36 to 31 Å in order to avoid strong steric clashes between the side chains belonging to different layers. This was done by using six MC simulations of 5×10^4 steps while such distance is decreased in 1 Å decrements. After this, an equilibration of 5×10^4 steps was performed in order to sample the setting angles. Finally, a MC simulation was run for a total of 2×10^5 steps and co-ordinates were saved every 2000 steps.

The Amber force-field [16] was used to represent the electrostatic, van der Waals and torsional energies of the system. Both methyl and methylene groups were described considering a model of united atoms and their van der Waals energy was computed in the usual pairwise additive way using a Lennard-Jones 6-12 potential. Electrostatic charges were determined by fitting the molecular electrostatic potential derived from quantum mechanical calculations to the classical one. Electrostatic interactions were evaluated using a standard Coulombic potential. Nonbonding interactions were truncated at 8 Å.

3. Results and discussion

In a first step, MC simulations were performed following the computational procedure described in Section 2, i.e. considering all the dihedral angles of the alkyl side chains as degrees of freedom. Inspection to the resulting microstructures revealed a predominantly disordered state of the inter-layer region (Fig. 3a). Such disorder is in opposition with what should be expected for the crystalline phase A,

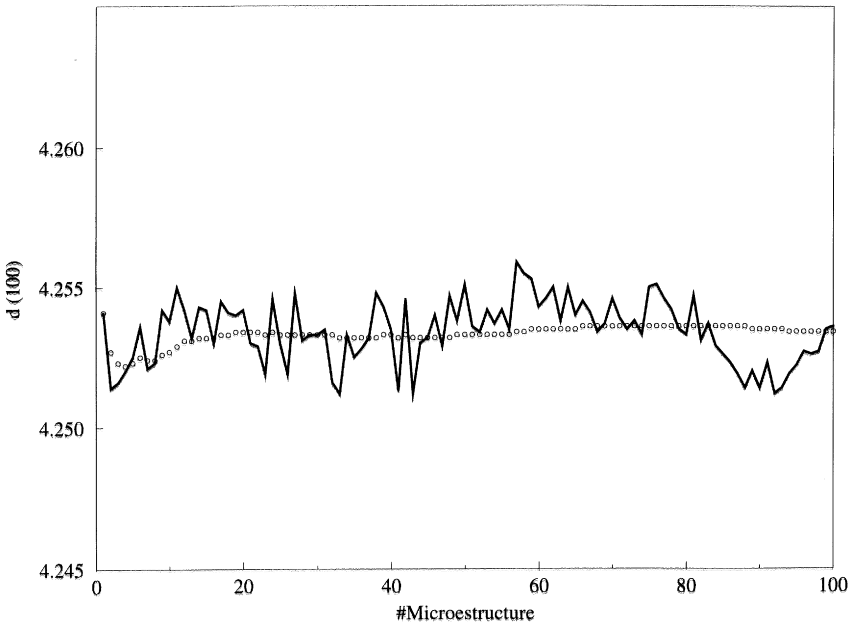

Fig. 4. Simulated spacing of the (100) reflection for each microstructure of PAALA-18 (solid line) as well as the running average along the simulation (dots).

which is conceived as an ordered state with a majority of the C–C bonds in the alkyl side chain adopting a *trans* conformation. This model is experimentally supported by both DSC and wide-angle X-ray scattering, which reflect crystallization of the paraffinic side chains. However, the side chains of the microstructures provided by MC simulations present a considerable number of C–C bonds in *gauche* conformation, which causes the side chains to be in a partially disordered state. Indeed, the results obtained from these simulations are essentially the same than those obtained when the phase B of PAALA-*n* with $n \geq 12$ was explicitly simulated [9].[2] Thus, the only order detected in Fig. 3a is the tendency of the side chains to align along the *b*-axis.

The failure to reproduce the crystallization of the paraffinic chains is due to the MC method by itself. It is known that MC simulations of alkanes below the experimental melting point lead to supercooled liquids rather than to crystals [17]. Since the goal of this work is to obtain a molecular model of the crystallized phase, we have constrained the conformation of some torsional angles of the alkyl side chains in order to facilitate the crystallization. Thus, the three central torsional angles included in the aliphatic segment that is not involved in the side chain bending were kept fixed at *trans*. CCB-MC simulations were run again using the computational procedure described in Section 2 but introducing the new constraints. It should be noted that these constraints should help in the crystallization process performing as a nucleus of the paraffin crystal lattice. In this case, simulations led to a highly ordered structure. Thus, the presence of order in the three axes allows to identify the phase A. Fig. 3b shows one of the microstructures generated from the latter simulations.

3.1. Structure and conformation of the alkyl side chains

The hexagonal arrangement of the alkyl side chains in PAALA-18 was evidenced in the electron diffraction diagrams obtained from casted thin films of this polymer [6]. In these diagrams as well as in the wide-angle region of the fibre X-ray diagrams, the (100) reflection with a spacing of 4.2 Å was observed. Accordingly, it was concluded that the side chains are separated within the hexagonal lattice by a distance of 4.2 Å/sin 60° = 4.9 Å. Fig. 4 shows the simulated spacing of the (100) reflection for each microstructure as well as the running average over the points. This spacing have been obtained from the distance between each side chain and its closest neighbours. For all the microstructures, the distances between one side chain and its six closest neighbours were very similar, the standard deviation associated to each dot represented in Fig. 4 being lower than 0.005 Å. As it can be seen, the spacing ranges from 4.251 and 4.255 Å along the simulation, this small variation being also consistent with a hexagonal pattern in which all the distances have the same value. On the other hand, the spacing obtained along the MC simulations is about 0.05 Å overestimated with respect to the experimental value. However, the average value of this spacing allows to estimate a distance between the side chains of 4.253 Å/sin 60° = 4.91 Å, which is in excellent agreement with the value derived using the experimental spacing.

Overall the results indicates that the hexagonal packing

[2] The phase B of PAALA-18 was investigated using MC simulations of the NPT type at 358 K. In those simulations the degrees of freedom were the torsional angles of the side chains and the length of the *b* edge of the cell.

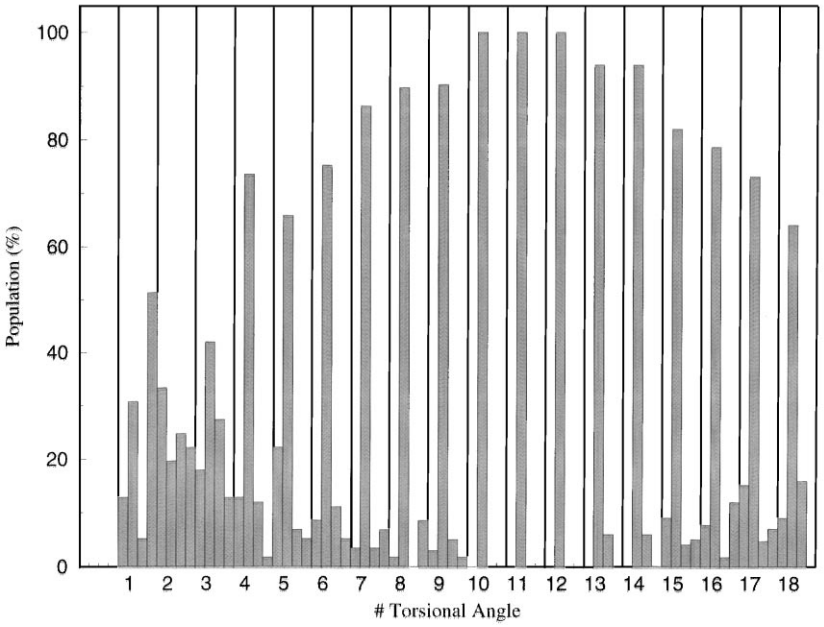

Fig. 5. Torsional angles distribution for the 13 residues contained in the helix repeat of PAALA-18. The population analysis of the torsional angle associated to each of the 18 bonds in the alkyl side chain is specified. The four categories considered for each bond, in the order displayed in the figure from left to right, are: *gauche*$^+$; *trans*; *gauche*$^-$; and the remaining conformers.

predicted by MC simulations for the side chains of PAALA-18 is in remarkable agreement with the available experimental information. According to this, it can be concluded that the structure displayed in Fig. 3b provides a very suitable description of the phase A of PAALA-18.

In order to get a deeper insight in the side chain structure, the corresponding torsional angles for the alkyl side chains of the 13 residues contained in the helix repeat of PAALA-18 were analyzed. Fig. 5 shows a population analysis for each torsional angle, the conformations being grouped in four categories: *gauche*$^-$; *trans*; *gauche*$^+$; and the remaining conformers. As it can be seen, the population of the folded states, i.e. those different from *trans*, is considerable for the first five torsional angles, even although the *trans* is, in general, the predominant conformation. This is not a surprising result since these torsional angles are involved

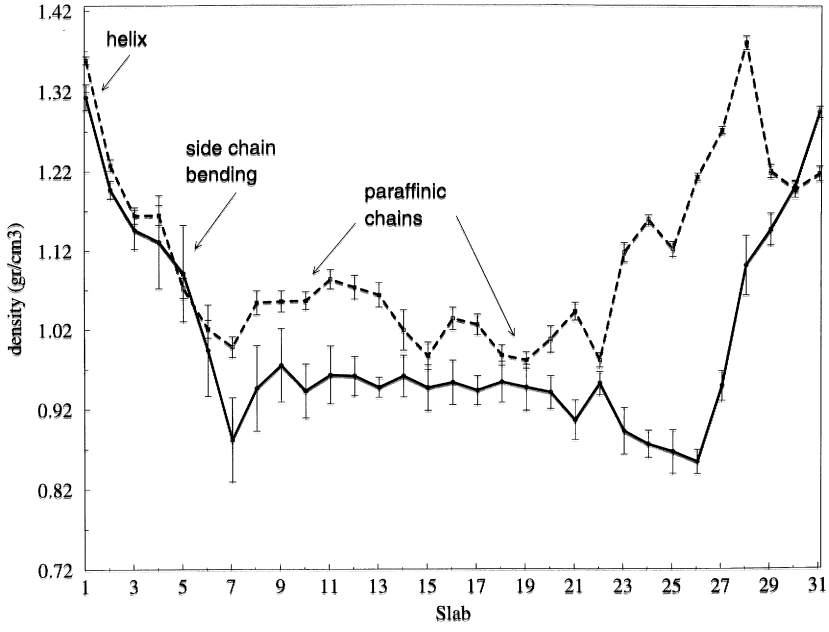

Fig. 6. Local density profiles of the phases A (solid line) and B (dashed line) of PAALA-18 along the *y*-axis.

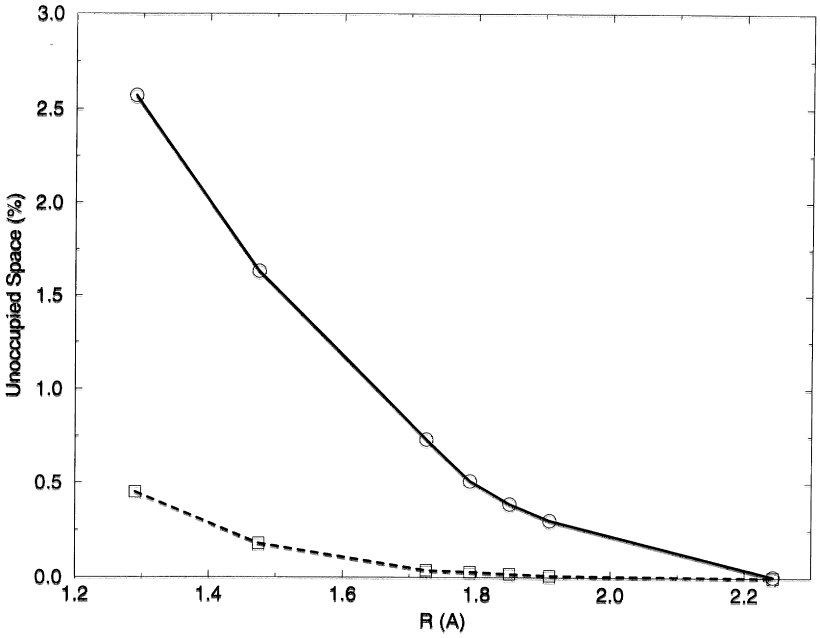

Fig. 7. Variation of the unoccupied space (in %) versus the radii of the prove particle (in Å) for the phases A (solid line) and B (dashed line) of PAALA-18.

in the side chain bending region, where the presence of folded conformations is required to orient the side chain perpendicular to the helix axis. On the other hand, for the 7th to the 15th torsional angles the population of the *trans* conformation is larger than 80% while that of the folded conformations is considerably small. As it was discussed above, the torsional angles 10th, 11th and 12th (Fig. 5) the conformation was kept fixed at *trans* along the simulations. However, it should be emphasized that although the remaining torsional angles were allowed to vary without any restriction, the *trans* conformation was finally adopted in all of them. These results indicate that once the nucleus of the crystal is built by fixing three torsional angles, the contiguous methylene units tend to crystallize spontaneously. Finally, the *trans* is clearly the predominant conformer for the 16th, 17th and 18th torsional angles. However, the populations of folded conformations increase with respect to those of the central segment of the alkyl side chain revealing a partial flexibility.

The experimental evidences available for the phase A of PAALA-18 reveal that the approximate number of crystallized methylenes is around 8 [6]. Starting from 3 torsional angles in *trans* conformation, the simulations evolved spontaneously to 9 torsional angles with such conformation. This feature points out the remarkable agreement between theoretical and experimental results. Thus, the method is perfectly capable of reproducing the phase A of PAALA's if the tendency to evolve towards a supercooled liquid is overcome by imposing the appropriate restrictions.

3.2. Density profile

The local density profile of phase A of PAALA-18 was calculated by adding the mass of all the atoms located in a given slab of the structure and dividing it by the volume of the slab. A total of 31 slabs with a thickness of 3 Å were built along the *y*-axis. The computed density profile is displayed in Fig. 6. The local density in the helix region was found to be clearly greater than in the paraffinic region. Thus, the density decreases from 1.31 to about 0.85–0.90 g/cm^3 along the *y*-axis. It is worth noting that the local density is quite homogeneous along all the interlayer paraffinic region indicating a similar mass distribution in both the side bending and the crystallized regions. The mass density of the paraffinic region is between that of a fully disordered liquid alkane, i.e. 0.76 g/cm^3 for liquid C_{18} at the same temperature, and a highly ordered alkane, i.e. 1.00 g/cm^3 for the orthorhombic crystal form of polyethylene.

The local density profile of the phase B of PAALA-18 has been computed using the microstructures obtained in previous MC simulations [7,9]. Results are included in Fig. 6 for comparison. As it can be seen the local density in the paraffinic pool of the phase B is about 0.15 g/cm^3 larger than that computed for the paraffinic region of the phase A. This result is in excellent agreement with the experimental observation. Thus, PAALA-*n* with $n \geq 12$ get denser as the transition temperature T_1 is raised. Accordingly, the observed densities for the phases A and B of PAALA-18 are 1.03 and 1.14 g/cm^3, respectively.

3.3. Measurement of the unoccupied space

The unoccupied space refers to the volume not occupied by the atoms of the system. The measurement of the unoccupied space is highly desirable since it allows to predict the behaviour of the system against small penetrants [7,15].

Unoccupied space estimations of the phases A and B of PAALA-18 were done by dividing the simulation box of every microstructure into a three-dimensional uniformly spaced grid. These grids consisted of 81,180 and 74,460 nodes for phases A and B, respectively. Then an spherical probe particle with a radius R was centred in each node and the distance to the nearest atom of the polymeric matrix was measured. If this distance was larger than the sum of the van der Waals radii of the probe particle and the polymer atom, the node was identified as unoccupied. Seven different radii R were chosen for the probe particle, which correspond to small gas penetrants: 1.29 (He); 1.475 (H_2); 1.725 (Ar); 1.79 (O_2); 1.849 (N_2); 1.909 (CH_4); and 2.243 Å (CO_2). The van der Waals radii of the polymer atoms were taken from Amber libraries [16].

The results derived from the analysis of the unoccupied space in all the generated microstructures are summarized in Fig. 7, which displays the amount of unoccupied space averaged over the 100 microstructures recorded for the phases A and B of PAALA-18. It can be seen that the amount of unoccupied space decreases when the phase A changes to phase B. This is a very reasonable result since the former has a lower density than the latter. Thus, even although the phase B is less ordered than the phase A the space is more filled in the former. An inspection to the microstructures of phases A and B of PAALA-18 has revealed that the phase A presents a considerable amount of unoccupied space around the region of side chain bending. The densification that accompanies the phase change lead to a drastic reduction of the unoccupied space in such region.

On the other hand, the results indicate that the unoccupied space decreases with the increase of the size of the probe particle, the space available being almost negligible for the larger ones. Moreover, the ratio between the unoccupied spaces estimated for the phases A and B increases with the size of the probe particle. Accordingly, the ratio change from 6 to 19 when the radius increases from 1.29 to 1.725 Å. This trend confirms that the space is more uniformly filled when the alkyl side chains are melt than when they are crystallized. Thus, in order that the quantity of unoccupied space reached a negligible value, i.e. lower than 0.25%, particles with a radius of approximately 1.975 and 1.45 Å are needed for the phases A and B of PAALA-18, respectively.

4. Conclusions

The structural behaviour of the phase A of PAALA-18 has been investigated using MC simulations. The results together with those obtained for the phase B of the same polymer provide a complete picture of the structural changes involved in the first thermal transition of PAALA-n with $n \geq 12$. The position of the alkyl side chains in the interhelical region predicts the crystallization of about 8–10 methylene groups. Furthermore, this paraffinic lattice adopts a hexagonal arrangement with the side chain separated by 4.9 Å and extended normal to the helix axis, in excellent agreement with the experimental data. The density profile obtained from our simulations indicates that the local density is quite homogeneous along all the interlayer region and much lower than that of the space occupied by the main chain helices. The side bending and the crystallized regions present a similar mass distribution in the phase A of PAALA-18. On the other hand, the phase B is denser than the phase A, the former offering a lower amount of unoccupied space than the latter.

Acknowledgements

This work was supported by DGICYT (PB96-0490). DZ and SL acknowledge the support of the Ministry of Education of Spain. AMN thanks financial support to FAPESP when in Spain. Authors thank to CESCA and CEPBA for computational facilities.

References

[1] Daly WH, Poché D, Negulescu II. Prog Polym Sci 1994;19:79.
[2] Watanabe J, Ono H, Uematsu I, Abe A. Macromolecules 1985;18:2141.
[3] Sakamoto R, Osawa A. Mol Cryst Liq Cryst 1987;153:385.
[4] Watanabe J, Nagase T. Macromolecules 1988;21:171.
[5] Romero Colomer FJ, Gómez Ribelles JL, Lloveras Macía J, Muñoz-Guerra S. Polymer 1991;32:1642.
[6] López-Carrasquero F, Montserrat S, Martínez de Ilarduya A, Muñoz-Guerra S. Macromolecules 1995;28:5535.
[7] Zanuy D, Alemán C, López-Carrasquero F, Báez ME, García-Alvarez M, Laso M, Muñoz-Guerra S. Macromol Chem Phys (in press).
[8] Navas JJ, Alemán C, López-Carrasquero F, Muñoz-Guerra S. Polymer 1997;38:3477.
[9] León S, Alemán C, Muñoz-Guerra S, Laso M. J Theor Comput Polym Sci 2000;10:177.
[10] Navas JJ, Alemán C, López-Carrasquero F. Macromolecules 1995;28:4487.
[11] López-Carrasquero F, García-Alvarez M, Navas JJ, Alemán C, Muñoz-Guerra S. Macromolecules 1996;29:8449.
[12] Broadhurst MG. J Res Natl Bur Stand 1962;66A:241.
[13] de Pablo JJ, Laso M, Suter UW. J Chem Phys 1992;96:6157.
[14] de Pablo JJ, Laso M, Suter UW. Macromolecules 1993;26:6180.
[15] Zanuy D, León S, Alemán C, Muñoz-Guerra S. Polymer 2000;41:4169.
[16] Weiner SJ, Kollman PA, Case DA, Singh UC, Ghio C, Alagona G, Profeta S, Weiner P. J Am Chem Soc 1984;106:765.
[17] Widmann AH, Laso M, Suter UW. J Chem Phys 1995;102:5761.